FIELD AND DEFORMATION EFFECTS IN $RbHSO_4$ FERROELECTRIC

A. S. Vdovych[1], R. R. Levitskii[1], I. R. Zachek[2]
[1] *Institute for Condensed Matter Physics of the National Academy of Sciences of Ukraine, 1, Svientsitskii St., UA–79011, Lviv, Ukraine,*
[2] *Lviv Polytechnic National University, 12, Bandery St., UA–79013, Lviv, Ukraine*

(Received 16 April 2020; in final form 14 May 2020; accepted 19 May 2020; published online 15 June 2020)

A modified four-sublattice pseudospin model for $RbHSO_4$ ferroelectric, which takes into account the piezoelectric coupling of the pseudospin subsystem with lattice strains, is proposed. The model also takes into account lowering of the symmetry of the crystal under the influence of shear stresses σ_4 and σ_6.

We have calculated, in the mean-field approximation, the spontaneous polarization and longitudinal dielectric permittivity of mechanically free and clamped crystals, their piezoelectric, elastic and thermal characteristics. The effects of hydrostatic and uniaxial pressure, shear stresses and longitudinal electric field on the phase transition and the physical characteristics of the crystal have been investigated. A satisfactory quantitative description of the corresponding experimental data has been obtained. The electrocaloric effect in the crystal has been studied as well.

Key words: ferroelectrics, dielectric permittivity, piezoelectric coefficients, pressure effect, electric field effect, electrocaloric effect.

DOI: https://doi.org/10.30970/jps.24.2702

I. INTRODUCTION

Investigation into the effect of mechanical stresses of different symmetry as well as the electric field effect on the physical properties of ferroelectrics allows us to deeper understand mechanisms of phase transitions in these materials as well as to search for new physical effects, which are not observed under zero pressure and zero external field.

The ferroelectric with hydrogen bonds $RbHSO_4$ is an example of a crystal where the pressure effects are essential. At temperature $T = 263.65$ K [1], a phase transition from a high-temperature paraelectric to a low-temperature ferroelectric phase takes place. The crystal has a monoclinic symmetry (space group $P2_1/c$ in the paraelectric phase, P/c in the ferroelectric phase) [2–4]. In contrast to many other ferroelectrics with hydrogen bonds where the phase transition is connected with proton ordering, in this crystal protons are already ordered in both phases. Besides, there are two types of sulphate groups: SO_4 $(1f)$ $(f = 1, \ldots, 4)$, which oscillate between two equilibrium positions; SO_4 $(2f)$, which occupy one position on the hydrogen bond [3, 4] (Fig. 1,a). The ordering of SO_4 $(1f)$ groups causes a phase transition into the ferroelectric phase with spontaneous polarization appearing along c-axis.

For a theoretical description of dielectric properties of $RbHSO_4$, we proposed a phenomenologic theory of Landau–Devonshire [5], as well as pseudospin models with asymmetric double-well potential [6–8], which describe the dielectric properties in the mean-field approximation.

Later in [9], based on a four-sublattice pseudospin model of Rochelle salt [10], we proposed an analogous four-sublattice pseudospin model of $RbHSO_4$ with an asymmetric double-well potential, which takes into account also the piezoelectric coupling of the pseudospin and lattice subsystems. This model allowed us to describe qualitatively elastic constants, the dielectric and thermal properties of the crystal, as well as dielectric properties of a deuterated $RbDSO_4$ crystal [11]. Based on this model, we described the effect of hydrostatic pressure on the phase transition and longitudinal dielectric permittivity of the $RbHSO_4$ crystal [12]; also an attempt was made

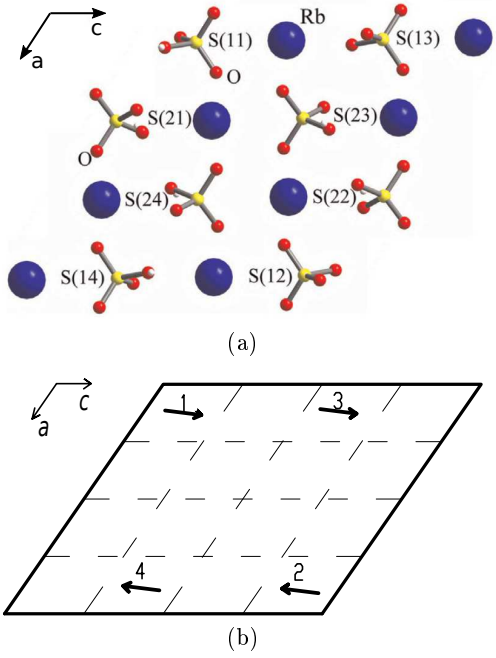

Fig. 1. Unit cell of $RbHSO_4$ (a) and schematic orientation of effective dipole moments $\mathbf{d}_{qf}$ of sulfate SO_4 $(1f)$ groups in paraelectric phase (b).

to predict the effect of uniaxial pressure and shear stress σ_5 on dielectric permittivity [12, 13]. However, the model [9] does not take into account the splitting of interaction parameters in the presence of shear strains ε_4 and ε_6, and can not predict the effect of shear stresses σ_4 and σ_6 on the thermodynamic characteristics of the crystal.

In the present paper, the model of $RbHSO_4$ [9] is modified to the case of lowering the symmetry under the influence of shear stresses σ_4 and σ_6. The effect of mechanical stresses of the different symmetry on the phase transition, dielectric, piezoelectric and thermal characteristics of the crystal has been investigated. Besides, the electric field effect on these characteristics as well as the electrocaloric effect have been investigated.

II. DEFORMED 4-SUBLATTICE MODEL

For the calculation of the thermodynamic characteristics of a $RbHSO_4$ crystal, we use model [9], taking into account four structure elements (sulfate groups $(SO_4)_{11}$, $(SO_4)_{12}$, $(SO_4)_{13}$, $(SO_4)_{14}$) in the unit cell, which moves in asymmetric double-well potentials.

Dipole moments $\mathbf{d}_{qf}$ are ascribed to these sulfate groups, where q is a serial number of a unit cell, f is a serial number of a dipole moment in the unit cell (f=1,...,4). In the paraelectric phase, the sum of these dipole moments is equal to zero, and their orientations are shown in Fig. 1,b. Changes in $\Delta\mathbf{d}_{qf}$ are responsible for the appearing of a spontaneous polarization in the ferroelectric phase.

Pseudospin variables $\frac{\sigma_{q1}}{2},\ldots,\frac{\sigma_{q4}}{2}$ describe the reorientation of the respective dipole moments of the base units: $\mathbf{d}_{qf}=\mu_f\frac{\sigma_{qf}}{2}$. Mean values $\langle\frac{\sigma}{2}\rangle=\frac{1}{2}(n_a-n_b)$ are connected with differences in the occupancy of the two possible molecular positions, n_a and n_b.

The Hamiltonian of the model in the pseudo-spin representation is

$$\hat{H}=NU_{\rm seed}-\frac{1}{2}\sum_{qq'}\sum_{f,f'=1}^{4}J_{ff'}(qq')\frac{\sigma_{qf}}{2}\frac{\sigma_{q'f'}}{2}$$
$$-\sum_{q}\sum_{f=1}^{4}(\Delta_f+\boldsymbol{\mu}_f\mathbf{E})\frac{\sigma_{qf}}{2}, \qquad (2.1)$$

where N is the total number of unit cells.

The term $U_{\rm seed}$ in (2.1) is "seed" energy, which relates to the heavy ion sublattice and does not explicitly depend on the configuration of the proton subsystem. It includes elastic, piezolectric and dielectric parts expressed in terms of electric fields E_i $(i=1,2,3)$ and strains u_j $(j=1,\ldots,6)$:

$$U_{\rm seed}=v\Big(\frac{1}{2}\sum_{j,j'=1}^{6}c^0_{jj'}(T)u_ju_{j'} \qquad (2.2)$$
$$-\sum_{i=1}^{3}\sum_{j=1}^{6}e^0_{ij}u_jE_i-\sum_{i,i'=1}^{3}\frac{1}{2}\chi^{u0}_{ii'}E_iE_{i'}\Big).$$

Parameters $c^0_{jj'}(T)$, e^0_{ij}, χ^{u0}_{ij} are the so called "seed" elastic constants, "seed" coefficients of piezoelectric stresses and "seed" dielectric susceptibility, respectively; v is the volume of a unit cell. Matrices $c^0_{jj'}(T)$, e^0_{ij}, $\chi^{u0}_{ii'}$ are given by:

$$\hat{c}^0_{jj'}=\begin{pmatrix} c^0_{11}(T) & c^0_{12}(T) & c^0_{13}(T) & 0 & c^0_{15}(T) & 0\\ c^0_{12}(T) & c^0_{22}(T) & c^0_{23}(T) & 0 & c^0_{25}(T) & 0\\ c^0_{13}(T) & c^0_{23}(T) & c^0_{12}(T) & 0 & c^0_{35}(T) & 0\\ 0 & 0 & 0 & c^0_{44}(T) & 0 & c^0_{46}(T)\\ c^0_{15}(T) & c^0_{25}(T) & c^0_{35}(T) & 0 & c^0_{55}(T) & 0\\ 0 & 0 & 0 & c^0_{46}(T) & 0 & c^0_{66}(T)\end{pmatrix}, \qquad (2.3)$$

$$\hat{e}^0_{ij}=\begin{pmatrix} e^0_{11} & e^0_{12} & e^0_{13} & 0 & e^0_{15} & 0\\ 0 & 0 & 0 & e^0_{24} & 0 & e^0_{26}\\ e^0_{31} & e^0_{32} & e^0_{33} & 0 & e^0_{35} & 0\end{pmatrix}, \qquad (2.4)$$

$$\hat{\chi}^{u0}_{ii'}=\begin{pmatrix} \chi^{u0}_{11} & 0 & \chi^{u0}_{13}\\ 0 & \chi^{u0}_{22} & 0\\ \chi^{u0}_{13} & 0 & \chi^{u0}_{33}\end{pmatrix}. \qquad (2.5)$$

The "seed" elastic constants $c^0_{jj}(T)$ are taken to be linearly dependent on temperature:

$$c^0_{jj'}(T)=c^0_{jj'}+k_{jj'}(T-T_{\rm c}). \qquad (2.6)$$

The coefficients $k_{jj'}$ phenomenologically take into account the high-temperature anharmonic lattice interactions. In the paraelectric phase, all coefficients $e^0_{ij}\equiv 0$.

The second term in (2.1) describes interactions between pseudospins; σ_{qf} is z-component of the pseudospin operator that describes the state of the pseudospin in the q-th cell on the sulfate group $(SO_4)_{1f}$ (f=1,2,3,4). Having done such identical transformation

$$\sigma_{qf}=\eta_f+(\sigma_{qf}-\eta_f),\quad \eta_f=\langle\sigma_{qf}\rangle, \qquad (2.7)$$

and neglecting quadratic fluctuations, the second term in (2.1) can be written in the mean field approximation:

$$-\frac{1}{2}\sum_{qq'}\sum_{f,f'=1}^{4}J_{ff'}(qq')\frac{\sigma_{qf}}{2}\frac{\sigma_{q'f'}}{2} \qquad (2.8)$$
$$=\frac{1}{2}\sum_{\substack{qq'\\ff'}}J_{ff'}(qq')\frac{\eta_f}{2}\frac{\eta_{f'}}{2}-\sum_{\substack{qq'\\ff'}}J_{ff'}(qq')\frac{\eta_{f'}}{2}\frac{\sigma_{qf}}{2}.$$

The third term in (2.1) describes interactions of the pseudospins with external electric field $\mathbf{E}$ and with local fields Δ_f. The parameters $\boldsymbol{\mu}_f$ are effective dipole moments per one pseudospin: $\boldsymbol{\mu}_1=\boldsymbol{\mu}_2=(\mu^x,\mu^y,\mu^z)$, $\boldsymbol{\mu}_3=\boldsymbol{\mu}_4=(\mu^x,-\mu^y,\mu^z)$.

Fourier transforms of the interaction constants $J_{ff'}=\sum\limits_{q'}J_{ff'}(qq')$ at $\mathbf{k}=0$, as well as local fields Δ_f are linearly expanded over the strains u_j:

$$J_{ff'}=J^0_{ff'}+\sum_j\psi_{ff'j}u_j,\ \Delta_f=\Delta^0_f+\sum_j\varphi_{fj}u_j. \qquad (2.9)$$

Taking into account the symmetry of the crystal, parameters $J_{ff'}$ are given by:

$$\begin{aligned}
J_{\frac{11}{22}} &= J^0_{11} + \sum_{l=1,2,3,5} \psi_{11l}u_l + \psi_{114}u_4 + \psi_{116}u_6,\\
J_{\frac{33}{44}} &= J^0_{11} + \sum_{l} \psi_{11l}u_l - \psi_{114}u_4 - \psi_{116}u_6, \quad (2.10)\\
J_{\frac{12}{34}} &= J^0_{12} + \sum_{l} \psi_{12l}u_l \pm \psi_{124}u_4 \pm \psi_{126}u_6,\\
J_{\frac{13}{24}} &= J^0_{13} + \sum_{l} \psi_{13l}u_l, J_{\frac{14}{23}} = J^0_{14} + \sum_{l} \psi_{14l}u_l,\\
\Delta_{\frac{1}{3}} &= \Delta^0_1 + \sum_{l} \varphi_{1l}u_l \pm \varphi_{14}u_4 \pm \varphi_{16}u_6,\\
\Delta_{\frac{2}{4}} &= -\Delta^0_1 - \sum_{l} \varphi_{1l}u_l \mp \varphi_{14}u_4 \mp \varphi_{16}u_6.
\end{aligned}$$

As a result, in the mean field approximation, the initial Hamiltonian (2.1) can be written as:

$$\hat{H} = NU_{\text{seed}} + \frac{N}{8}\sum_{ff'} J_{ff'}\eta_f\eta_{f'} - \sum_q \sum_{f=1}^{4} \mathcal{H}_f \frac{\sigma_{qf}}{2}, \quad (2.11)$$

where

$$\mathcal{H}_f = \left(\frac{1}{2}\sum_{f'} J_{ff'}\eta_{f'} + \Delta_f + \boldsymbol{\mu}_f \mathbf{E}\right). \quad (2.12)$$

III. THERMODYNAMIC CHARACTERISTICS OF $RbHSO_4$

For the calculation of the thermodynamic characteristics of $RbHSO_4$, we use the thermodynamic potential per unit cell, which is obtained in the mean field approximation:

$$\begin{aligned}
g = \frac{G}{N} &= U_{\text{seed}} + \frac{1}{8}\sum_{ff'} J_{ff'}\eta_f\eta_{f'} \quad (3.1)\\
&-4\frac{1}{\beta}\ln 2 - \frac{1}{\beta}\sum_{f=1}^{4} \ln\cosh\frac{\beta}{2}\mathcal{H}_f - v\sum_{j=1}^{6}\sigma_j u_j.
\end{aligned}$$

Using equilibrium condition

$$\left(\frac{\partial g}{\partial \eta_f}\right)_{E_i,\sigma_i} = 0, \quad \left(\frac{\partial g}{\partial u_j}\right)_{E_i,\sigma_i} = 0$$

we obtain equations for order parameters η_f and strains u_j:

$$\eta_f = \tanh\frac{\beta}{2}\mathcal{H}_f. \quad (3.2)$$

$$\begin{aligned}
\sigma_j &= \sum_{j'=1}^{6} c^0_{jj'}(T)u_{j'} - \sum_{i=1}^{3} e^0_{ij}E_i \quad (3.3)\\
&- \sum_{f,f'=1}^{4} \frac{\psi_{ff'j}}{8v}\eta_f\eta_{f'} - \sum_{f=1}^{4}\frac{\varphi_{fj}}{2v}\eta_f.
\end{aligned}$$

On the basis of thermodynamic potential (3.1), we get expressions for different thermodynamic characteristics. Expressions for components of the polarization vector are as follows:

$$\begin{aligned}
P_i &= -\frac{1}{v}\left(\frac{\partial g}{\partial E_i}\right) \quad (3.4)\\
&= \sum_{j=1}^{6} e^0_{ij}u_j + \sum_{i'=1}^{3}\chi^{u0}_{ii'}E_{i'} + \frac{1}{2v}\sum_{f=1}^{4}\mu^{(i)}_f\eta_f.
\end{aligned}$$

Isothermic dielectric susceptibility of a mechanically clamped crystal is given by:

$$\chi^u_{ii'} = \left(\frac{\partial P_i}{\partial E_{i'}}\right)_{u_j} = \chi^{u0}_{ii'} + \frac{1}{2v}\sum_{f=1}^{4}\mu^{(i)}_f\eta'_{E_{i'}f}. \quad (3.5)$$

In order to determine $\eta'_{E_{i'}f}$, we differentiate the system of equations (3.2) over field E_i:

$$\hat{I}\eta'_{E_i} = \hat{A}^\eta\eta'_{E_i} + \mathbf{A}^{E_i} \;\Rightarrow\; \eta'_{E_i} = -(\hat{A}^\eta - \hat{I})^{-1}\mathbf{A}^{E_i}, \quad (3.6)$$

where $\hat{I}$ is identity matrix, the coefficients of matrix $\hat{A}^\eta$ and vector $\mathbf{A}^{E_i}$ are as follow:

$$\begin{aligned}
A^\eta_{ff'} &= \frac{\beta}{4}J_{ff'}\left(1 - \tanh^2\frac{\beta}{2}\mathcal{H}_f\right) = \frac{\beta}{4}J_{ff'}(1-\eta^2_f),\\
A^{E_i}_f &= \frac{\beta}{2}\mu^{(i)}_f(1-\eta^2_f). \quad (3.7)
\end{aligned}$$

Coefficients of piezoelectric stress are given by:

$$e_{ij} = \left(\frac{\partial P_i}{\partial u_j}\right)_{E_i} = e^0_{ij} + \frac{1}{2v}\sum_{f=1}^{4}\mu^{(i)}_f\eta'_{u_jf}. \quad (3.8)$$

In order to determine η'_{u_jf}, we differentiate the system of equations (3.2) over strain u_j:

$$\hat{I}\eta'_{u_j} = \hat{A}^\eta\eta'_{u_j} + \mathbf{A}^{u_j} \;\Rightarrow\; \eta'_{u_j} = -(\hat{A}^\eta - \hat{I})^{-1}\mathbf{A}^{u_j}, \quad (3.9)$$

where the coefficients of vector $\mathbf{A}^{u_j}$ are as follow:

$$A^{u_j}_f = \frac{\beta}{2}\mathcal{H}^u_{fj}(1-\eta^2_f), \;\; \mathcal{H}^u_{fj} = \frac{1}{2}\sum_{f'}\psi_{ff'j}\eta_{f'} + \varphi_{fj}. \quad (3.10)$$

Elastic constants in a constant field are as follows:

$$c_{jj'} = \left(\frac{\partial\sigma_j}{\partial u_{j'}}\right)_{E_i} = c^{E_i}_{jj'} - \frac{1}{2v}\sum_{f=1}^{4}\mathcal{H}^u_{fj}\eta'_{u_{j'}f}. \quad (3.11)$$

Molar entropy of the proton subsystem is:

$$\begin{aligned}
S &= -\frac{N_{\text{A}}}{N_{\text{m}}}\left(\frac{dg}{dT}\right)_{E_i,\sigma_j} = \frac{R}{N_{\text{m}}}\Bigg(-\frac{v}{2}\sum_{j,j'=1}^{6}k_{jj'}u_ju_{j'} \quad (3.12)\\
&+4\ln 2 + \sum_{f=1}^{4}\left(\ln\cosh\frac{\beta}{2}\mathcal{H}_f - \frac{\beta}{2}\mathcal{H}_f\tanh\frac{\beta}{2}\mathcal{H}_f\right)\Bigg),
\end{aligned}$$

Here N_{A} is the Avogadro constant, R is the gas constant, $N_{\text{m}} = 8$ is the number of molecules $RbHSO_4$ in the unit cell.

Molar heat capacity of the proton subsystem is:

$$\Delta C = T\left(\frac{dS}{dT}\right)_{E_i,\sigma_j} = T\Big(\sum_{f=1}^{4} S'_{\eta_f}\eta'_{Tf} + \sum_{j=1}^{6} S'_{u_j}u'_{Tj} + S'_T\Big), \tag{3.13}$$

where such notations are used:

$$S'_{\eta_f} = -\frac{R}{N_{\rm m}}\frac{\beta^2}{4}\sum_{f'=1}^{4}\mathcal{H}_{f'}(1-\eta_{f'}^2)\frac{1}{2}J_{ff'}, \tag{3.14}$$

$$S'_{u_j} = \frac{R}{N_{\rm m}}\Big(-v\sum_{j'=1}^{6}k_{jj'}u_{j'} - \frac{\beta^2}{4}\sum_{f=1}^{4}\mathcal{H}_f(1-\eta_f^2)\mathcal{H}^u_{fj}\Big),$$

$$S'_T = \frac{R}{N_{\rm m}}\frac{\beta^2}{4T}\sum_{f=1}^{4}\mathcal{H}_f^2(1-\eta_f^2),$$

In order to determine η'_{Tf} and u'_{Tj}, we differentiate the system of equations (3.2), (3.3) over temperature:

$$\begin{pmatrix}\hat{A}^\eta - \hat{I} & \hat{A}^u\\ \hat{B}^\eta & \hat{c}^0\end{pmatrix}\begin{pmatrix}\eta'_T\\ \mathbf{u}'_T\end{pmatrix} + \begin{pmatrix}\mathbf{A}^T\\ \mathbf{B}^T\end{pmatrix} = \mathbf{0} \tag{3.15}$$

$$\Rightarrow \begin{pmatrix}\eta'_T\\ \mathbf{u}'_T\end{pmatrix} = -\begin{pmatrix}\hat{A}^\eta - \hat{I} & \hat{A}^u\\ \hat{B}^\eta & \hat{c}^0\end{pmatrix}^{-1}\begin{pmatrix}\mathbf{A}^T\\ \mathbf{B}^T\end{pmatrix}.$$

where such notations are used:

$$A^u_{fj} = \frac{\beta}{2}\mathcal{H}^u_{fj}(1-\eta_f^2), \quad B^\eta_{jf} = -\frac{1}{2v}\mathcal{H}^u_{fj}.$$

$$A^T_f = -\frac{\mathcal{H}_f(1-\eta_f^2)}{2k_BT^2}, \quad B^T_j = \sum_{j'=1}^{6}k_{jj'}u_{j'}. \tag{3.16}$$

The total specific heat is considered to be the sum of the proton and lattice contributions:

$$C = \Delta C + C_{\rm lattice}. \tag{3.17}$$

The lattice contribution near $T_{\rm c}$ is approximated by the linear dependence

$$C_{\rm lattice} = C_0 + C_1(T - T_{\rm c}). \tag{3.18}$$

The corresponding lattice contribution to the entropy near $T_{\rm c}$ then is:

$$S_{\rm lattice} = \int\frac{C_{\rm lattice}}{T}\,dT = (C_0 - C_1T_{\rm c})\ln(T) + C_1T + \text{const}. \tag{3.19}$$

Hence, the total entropy as a function of temperature and a component of field E_3 is

$$S_{\rm total}(T, E_3) = S + S_{\rm lattice}. \tag{3.20}$$

Solving (3.20) with respect to temperature at $S_{\rm total}(T, E_3)$ = const and two values of the field, one can calculate the electrocaloric temperature shift (as seen in Fig. 15)

$$\Delta T_{\rm ec} = T(S_{\rm total}, E_3(2)) - T(S_{\rm total}, E_3(1)). \tag{3.21}$$

The electrocaloric temperature change can be calculated also using the known formula

$$\Delta T_{\rm ec} = -\int_0^{E_3}\frac{TV}{C}\left(\frac{\partial P_3}{\partial T}\right)_{E,\sigma}dE_3, \tag{3.22}$$

where piroelectric coefficient

$$\left(\frac{\partial P_3}{\partial T}\right)_{E,\sigma} = \sum_{j=1}^{6}e^0_{3j}u'_{Tj} + \frac{1}{2v}\sum_{f=1}^{4}\mu^z_f\eta'_{Tf}, \tag{3.23}$$

$V = vN_{\rm A}/4$ is the molar volume.

IV. COMPARISON OF THE THEORETICAL RESULTS WITH THE EXPERIMENTAL DATA. DISCUSSION.

The theory parameters are determined from the condition of agreement of the calculated characteristics with the experimental data for the temperature dependences of spontaneous polarization $P_3(T)$ [2, 14], dielectric permittivity $\varepsilon_{33}(T)$ in the absence of external influences [2, 14, 15] and at different values of hydrostatic pressure [1] and of electric field [5], molar heat capacity $C(T)$ [16] and elastic constants $c_{jj'}(T)$ [15].

To determine the theoretical parameters, it is necessary to use the dependence of temperature $T_{\rm c}$ on hydrostatic pressure $T_{\rm c}(p_{\rm h})$ [1]. Unfortunately, different authors propose different values for $T_{\rm c}(0)$: from 258.15 K [2] to 265.25 K [5]. Further we "will be attached" to $T_{\rm c}(0)$ = 263.65 K [1].

Parameters of the interactions between pseudospins at zero values of strains $J^0_{ff'}$ $(f, f' = 1, 2, 3, 4)$ and local fields Δ^0_f, which cause the asymmetry in the occupation of the two positions, mainly fix the phase transition temperature from a paraelectric to a ferroelectric phase in the absence of external pressure and field, the order of phase transition and the shape of curves $P_3(T)$, $\varepsilon_{33}(T)$ and $C(T)$. Their optimal values are: $J^0_{11}/k_{\rm B}$=$J^0_{13}/k_{\rm B}$ = 372,K, $J^0_{12}/k_{\rm B}$=$J^0_{14}/k_{\rm B}$ = 310 K, $\Delta^0_1/k_{\rm B}$ = 244.81 K.

Deformational potentials $\psi_{ff'j}$ and φ_{fj} [see 2.9)] mainly fix the temperature dependences of spontaneous strains u_j, piezoelectric coefficients and elastic constants, as well as the shift of the phase transition temperature under mechanical stresses. The optimal values of the deformational potentials are:

$\tilde{\psi}_{111} = -1700$ K, $\tilde{\psi}_{112} = -4600$ K, $\tilde{\psi}_{113} = -500$ K,

$\tilde{\psi}_{114} = 0$ K, $\tilde{\psi}_{115} = 1200$ K, $\tilde{\psi}_{116} = 3500$ K,

$\tilde{\psi}_{121} = -500$ K, $\tilde{\psi}_{122} = -3040$ K, $\tilde{\psi}_{123} = -500$ K,

$\tilde{\psi}_{124} = 0$ K, $\tilde{\psi}_{125} = 400$ K, $\tilde{\psi}_{126}/k_{\rm B} = -7000$ K,

$\tilde{\psi}_{ff'j} = \psi_{ff'j}/k_{\rm B}$.

A numerical analysis shows that the thermodynamic characteristics depend on the following sums: $\psi_{11l}+\psi_{13l}$, $\psi_{12l}+\psi_{14l}$ (l=1,2,3,5). Therefore, for the sake of simplicity we chose them to be equal, that is $\psi_{13l}=\psi_{11l}$, $\psi_{14l}=\psi_{12l}$. The rest of the parameters $\psi_{ff'j}$ can be determined from the symmetry of crystal $RbHSO_4$, as it is written in (2.10). Parameters φ_{fj} influence the thermodynamic characteristics practically in the same way, as simply renormalized parameters $\psi_{ff'j}$. Therefore, for the sake of simplicity, we chose them to be $\varphi_{fj}=0\,\mathrm{K}$.

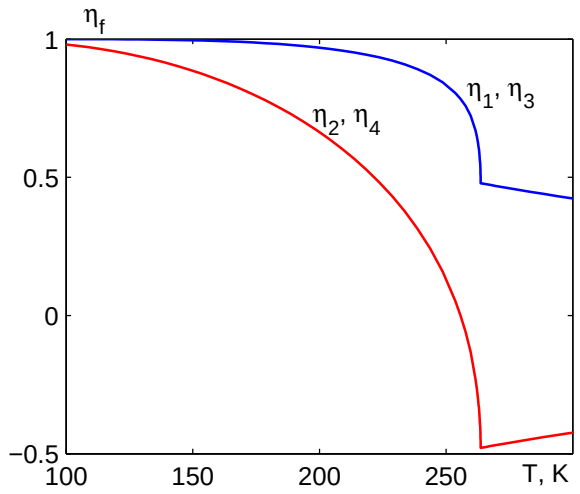

Fig. 2. Temperature dependence of order parameters η_f.

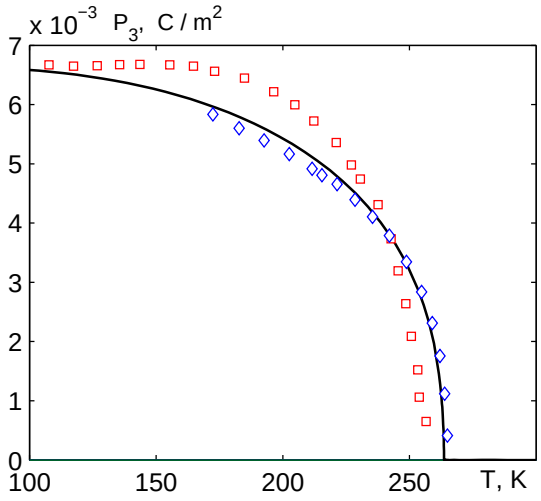

Fig. 3. Temperature dependence of spontaneous polarization. Symbols are experimental data of [14] (◇), [2] (□).

The components of effective dipole moments μ^x, μ^y, μ^z are found from the condition of agreement between theory and experiment for the corresponding components of spontaneous polarization and dielectric permittivity. The optimal value of the longitudinal component is $\mu^z = 2.8\cdot10^{-30}\,\mathrm{C\cdot m}$. Since the symmetry of the crystal permits existence of the transverse component of spontaneous polarization P_x, but experimentally it is absent or very

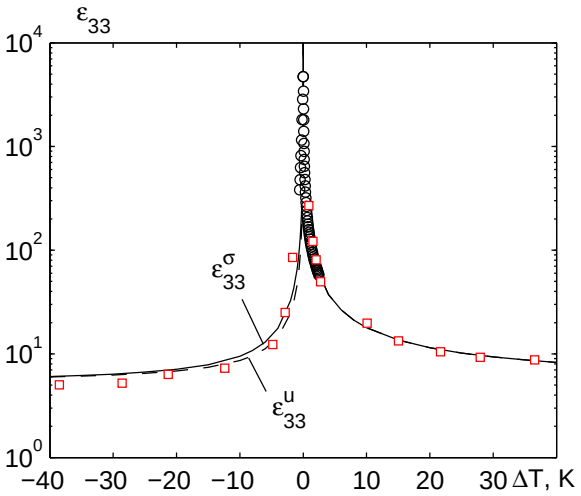

Fig. 4. Temperature dependences of dielectric permittivity of the mechanically free $\varepsilon^{\sigma}_{33}$ and clamped ε^{u}_{33} crystal. Symbols are experimental data of [5] (○), [2] (□).

small, then parameter $\mu^x = 0.0\,\mathrm{C\cdot m}$. The symmetry of the crystal forbids existence of the transverse component P_y, because, as was said above, $\boldsymbol{\mu}_1=\boldsymbol{\mu}_2=(\mu^x,\mu^y,\mu^z)$, $\boldsymbol{\mu}_3=\boldsymbol{\mu}_4=(\mu^x,-\mu^y,\mu^z)$, and contributions to polarization P_y compensate each other in pairs (μ^y_1 with μ^y_3 and μ^y_2 with μ^y_4). To determine the component μ^y, one could use some experimental data for the component of dielectric permittivity ε_{22}. However, this permittivity is measured only at one temperature; and this is not enough to separate the pseudospin and lattice contributions into permittivity. Further, we assume that the pseudospin contribution into ε_{22} is absent, and then $\mu^y = 0.0\,\mathrm{C\cdot m}$.

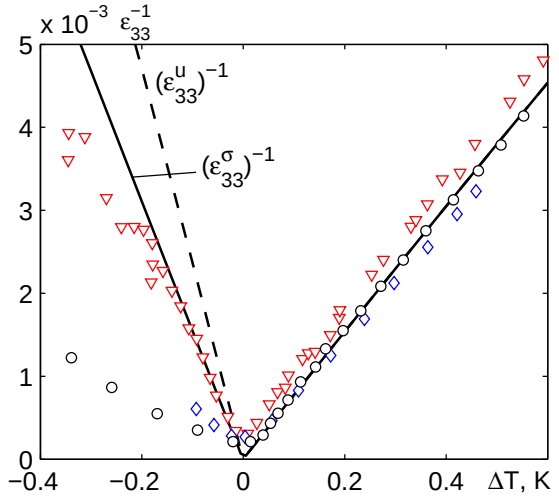

Fig. 5. Temperature dependences of the inverse dielectric permittivity of mechanically free $(\varepsilon^{\sigma}_{33})^{-1}$ and clamped $(\varepsilon^{u}_{33})^{-1}$ crystal. Symbols are experimental data of [5] (○), [14] (◇), [15] (▽).

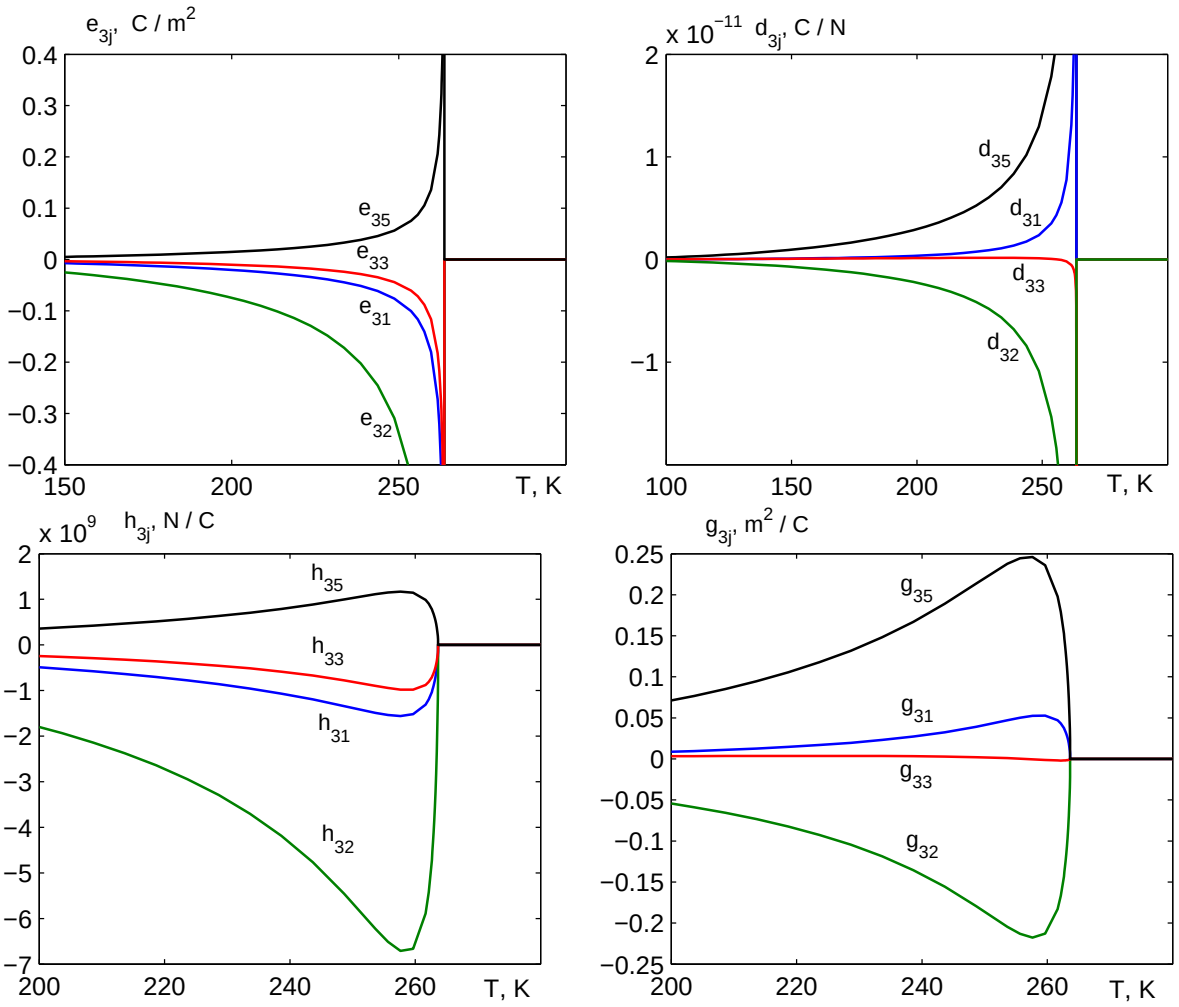

Fig. 6. The temperature dependences of piezoelectric coefficients e_{3j}, d_{3j}, h_{3j}, g_{3j}.

The "seed" dielectric susceptibility $\chi^{u0}_{ii'}$, coefficients of piezoelectric stress e^0_{ij} and elastic constants c^0_{ij} are found from the condition of agreement between theory and experiment in the temperature regions far from the phase transition temperature T_c. Their values are obtained as follows:

$$\chi^{u0}_{11} = 0.301, \quad \chi^{u0}_{22} = 0.403, \quad \chi^{u0}_{33} = 0.35, \quad \chi^{u0}_{13} = 0.0; \quad e^0_{ij} = 0\,\frac{\mathrm{C}}{\mathrm{m}^2};$$

$$c^0_{11} = 3.06 \cdot 10^{10}\,\frac{\mathrm{N}}{\mathrm{m}^2}, \quad c^0_{12} = 1.54 \cdot 10^{10}\,\frac{\mathrm{N}}{\mathrm{m}^2}, \quad c^0_{13} = 0.8 \cdot 10^{10}\,\frac{\mathrm{N}}{\mathrm{m}^2},$$

$$c^0_{22} = 3.8 \cdot 10^{10}\,\frac{\mathrm{N}}{\mathrm{m}^2}, \quad c^0_{23} = 0.67 \cdot 10^{10}\,\frac{\mathrm{N}}{\mathrm{m}^2}, \quad c^0_{33} = 3.62 \cdot 10^{10}\,\frac{\mathrm{N}}{\mathrm{m}^2},$$

$$c^0_{44} = 0.48 \cdot 10^{10}\,\frac{\mathrm{N}}{\mathrm{m}^2}, \quad c^0_{55} = 0.53 \cdot 10^{10}\,\frac{\mathrm{N}}{\mathrm{m}^2}, \quad c^0_{66} = 1.25 \cdot 10^{10}\,\frac{\mathrm{N}}{\mathrm{m}^2},$$

$$c^0_{15} = c^0_{25} = c^0_{35} = c^0_{46} = 0.0\,\frac{\mathrm{N}}{\mathrm{m}^2},$$

$$k_{11} = -37 \cdot 10^6\,\frac{\mathrm{N}}{\mathrm{m}^2 \cdot \mathrm{K}}, \quad k_{12} = -2 \cdot 10^6\,\frac{\mathrm{N}}{\mathrm{m}^2 \cdot \mathrm{K}}, \quad k_{13} = -10 \cdot 10^6\,\frac{\mathrm{N}}{\mathrm{m}^2 \cdot \mathrm{K}},$$

$$k_{22} = -10 \cdot 10^6\,\frac{\mathrm{N}}{\mathrm{m}^2 \cdot \mathrm{K}}, \quad k_{23} = -30 \cdot 10^6\,\frac{\mathrm{N}}{\mathrm{m}^2 \cdot \mathrm{K}}, \quad k_{33} = -42 \cdot 10^6\,\frac{\mathrm{N}}{\mathrm{m}^2 \cdot \mathrm{K}},$$

$$k_{44} = -5 \cdot 10^6\,\frac{\mathrm{N}}{\mathrm{m}^2 \cdot \mathrm{K}}, \quad k_{55} = -2 \cdot 10^6\,\frac{\mathrm{N}}{\mathrm{m}^2 \cdot \mathrm{K}}, \quad k_{66} = -27 \cdot 10^6\,\frac{\mathrm{N}}{\mathrm{m}^2 \cdot \mathrm{K}}.$$

The volume of a unit cell is $v = 0.842 \cdot 10^{-27}$ m^3.

Now let us focus on the obtained results. At low temperatures $T \ll T_c$ all pseudospins are ordered in the same direction, that is $\eta_f \to 1$ (Fig. 2), because all parameters of interaction $J^0_{ff'} > 0$. Then the spontaneous polarization tends to saturation (Fig. 3).

When temperature increases, the pseudospins disorder, that is parameters η_f, decreases. As a result, the effective mean field $\frac{1}{2}\sum\limits_{f'} J_{ff'}\eta_{f'}$ decreases [see (2.12)]. However, local fields $\Delta^0_1 = \Delta^0_3 = -\Delta^0_2 = -\Delta^0_4$ do not depend on temperature and cause a stronger disordering of sublattices "2" and "4" in comparison with "1" and "3". At temperature T_c, the second order phase transition takes place. Then the effective mean field $\frac{1}{2}\sum\limits_{f'} J_{ff'}\eta_{f'}$ disappears, but there remain only local fields Δ^0_f, which cause antiparallel ordering of pseudospins ($\eta_1 = \eta_3 = -\eta_2 = -\eta_4$). Near T_c the spontaneous polarization monotonically and continuously decreases as the temperature increases and goes to zero at the T_c point, the longitudinal dielectric permittivities of the mechanically free ε^σ_{33} and clamped ε^u_{33} crystal go to infinity at temperature T_c (Fig. 4), and corresponding inverse permittivities $(\varepsilon^\sigma_{33})^{-1}$ and $(\varepsilon^u_{33})^{-1}$ tend to zero (Fig. 5).

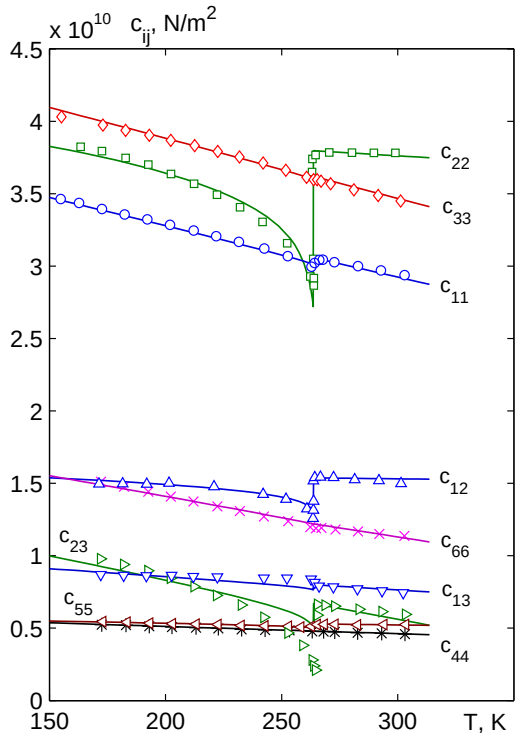

Fig. 7. The temperature dependences of elastic constants $c_{jj'}$. Symbols are experimental data of [15].

Piezoelectric coefficients are nonzero only in the ferroelectric phase (Fig. 6), coefficients e_{3j} and d_{3j} in absolute value go to infinity at the temperature T_c, whereas h_{3j} and g_{3j} are finite and continuously go to zero at the T_c point. Unfortunately, there are no experimental data for piezoelectric coefficients.

Temperature dependences of elastic constants (Fig. 7) and molar heat capacity (Fig. 8) have finite breaks in the T_c point.

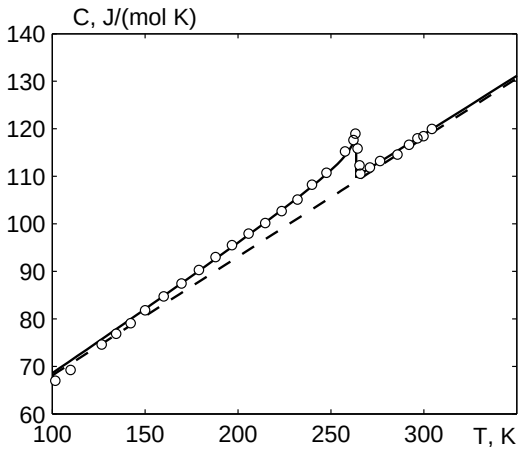

Fig. 8. The temperature dependence of molar heat capacity. Symbols are experimental data of [16] (○). Dashed line is lattice contribution, approximated by straight line.

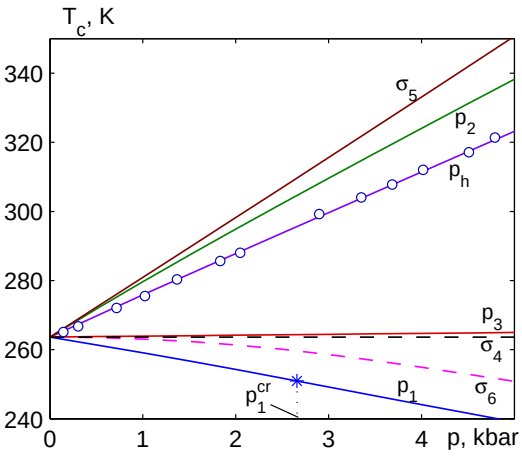

Fig. 9. Dependence of transition temperature T_c of the $RbHSO_4$ crystal on hydrostatic pressure p_h, ○ [1]; on uniaxial pressures: p_1, p_2, p_3; and on shear stresses σ_4, σ_5, σ_6.

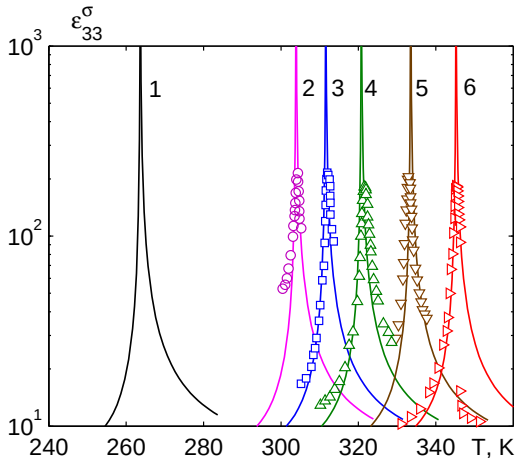

Fig. 10. Temperature dependence of dielectric permittivity of the mechanically free ε^σ_{33} crystal at the presence of hydrostatic pressure p_h (kbar): 0.0 — 1; 3.36 — 2, ○; 4.01 — 3, □; 4.79 — 4, △; 5.87 — 5, ▽; 6.85 — 6 ▷. Symbols are experimental data of [1].

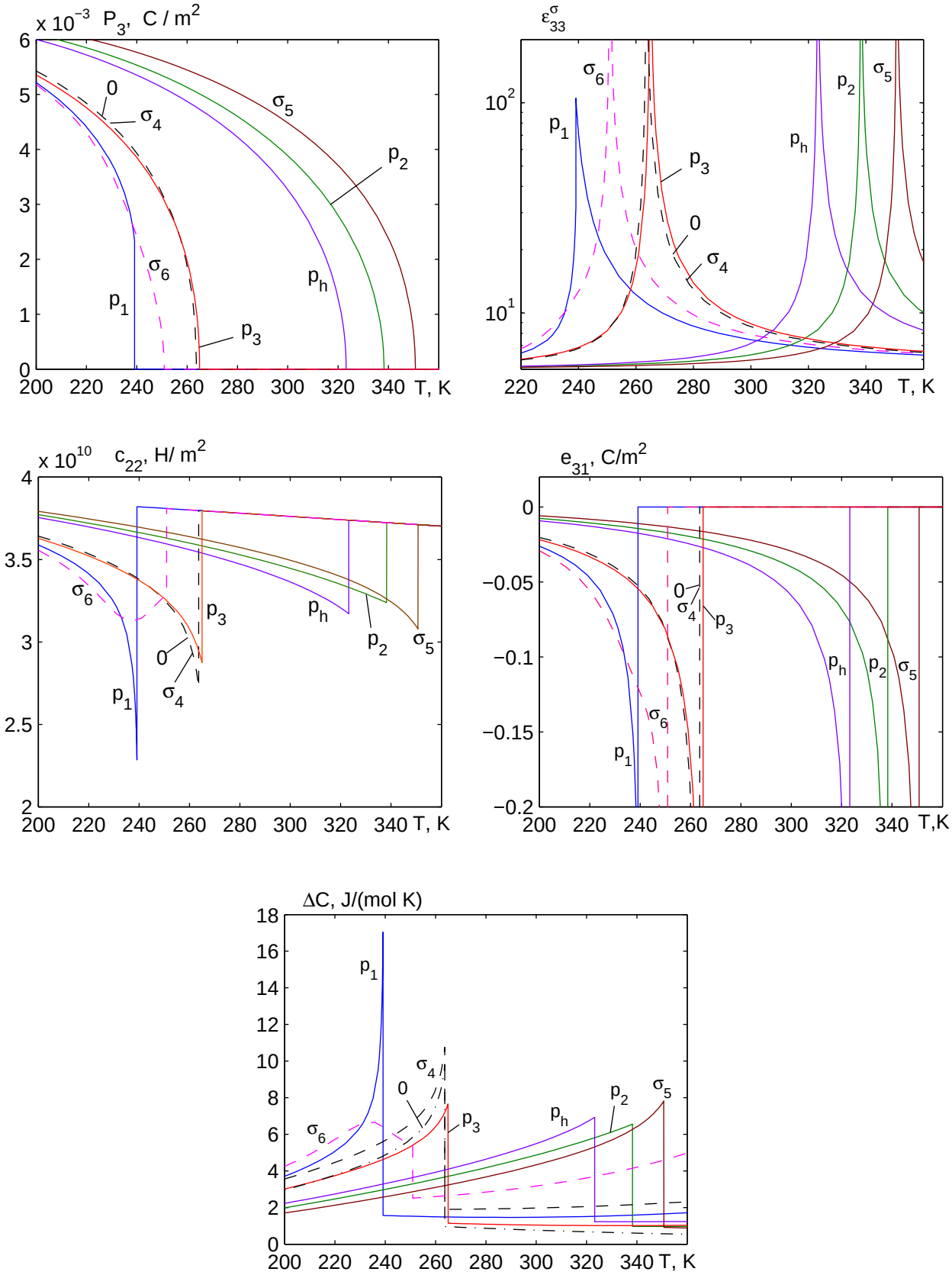

Fig. 11. Temperature dependences of spontaneous polarization P_3, dielectric permittivity of the mechanically free crystal $\varepsilon^{\sigma}_{33}$, elastic constant c_{22}, piezoelectric constant e_{31} and proton contribution to molar heat capacity ΔC in the presence of hydrostatic pressure $p_{\rm h}$, uniaxial pressure p_1, p_2, p_3 and shear stresses σ_4, σ_5, σ_6 5 kbar in magnitude. Curve 0 corresponds to zero stress.

As one can see from these figures, the calculated temperature dependences satisfactorily agree with the corresponding experimental data.

It is necessary to note that the temperature dependences of $P_3(T)$, $\varepsilon_{33}^{\sigma,u}(T)$, $\Delta C(T)$ shown above virtually coincide with the analogous curves calculated in [9] in the absence of mechanical stresses and an electric field.

The effect of mechanical stresses mainly reveals itself through the shift of temperature T_c (Fig. 9).

Note that the phase transition temperature practically linearly depends on the stresses which do not change the symmetry of the crystal, that is on the hydrostatic p_h and uniaxial p_1, p_2, p_3 pressures, as well as on the shear stress σ_5. The temperature dependences of the thermodynamic characteristics at these stresses (except for p_1) are qualitatively similar, as in the case of absence of stresses, in particular, curves $\varepsilon_{33}^{\sigma}(T)$ at different values of hydrostatic pressure p_h (Fig. 10), as well as curves $P_3(T)$, $\varepsilon_{33}^{\sigma}(T)$, $c_{22}(T)$, $e_{31}(T)$ $\Delta C(T)$ at mentioned above stresses 5 kbar in magnitude (Fig. 11, curves p_h, p_2, p_3, σ_5).

The dependence of transition temperature T_c on hydrostatic pressure p_h (Fig. 9, curve p_h), as well as temperature dependences $\varepsilon_{33}^{\sigma}$ at different values of p_h (Fig. 10) well agree with analogous curves, calculated in [12].

Uniaxial pressure p_1 has a different influence. At small values of p_1, the phase transition remains the second order one, and the temperature dependences of the thermodynamic characteristics are qualitatively similar as in the case of absence of pressure; in particular, one can see this on the temperature dependences $P_3(T)$ and $\varepsilon_{33}^{\sigma}(T)$ at different values of uniaxial pressure p_1 (Fig. 12, curves 0, 1, 2). Starting from some critical pressure p_1^{cr}=2.66 kbar (tricritical point), the phase transition becomes the first order one. As a result, at $p_1 > p_1^{cr}$ there are finite breaks on the curves of the temperature dependences of thermodynamic characteristics (Fig. 12, curves 3, 4, 5 and Fig. 11, curves p_1).

Shear stress σ_4 does not influence thermodynamic characteristics, and in Fig. 11, curves σ_4 coinside with curves 0, since deformational potentials $\psi_{ff'4} = 0$ K. The pseudospin contribution to molar heat capacity ΔC is an exception, in Fig. 11 curve σ_4 (solid line) does not coinside with curve 0 (dashed line). This is connected with temperature dependences of "seed" elastic constants $c_{jj'}^0(T)$; as a result, terms $-vk_{jj'}u_{j'}$ appear in expression S'_{u_j} [see (3.15)].

Shear stress σ_6 changes the symmetry of the crystal and, in contrast to other stresses, lowers the temperature T_c nearly quadratically, but not linearly (Fig. 9, curve σ_6). In this case, the phase transition remains the second order one. In addition to lowering the T_c point, the curves of temperature dependences $P_3(T)$, $\varepsilon_{33}^{\sigma}(T)$, $c_{22}(T)$, $e_{31}(T)$ $\Delta C(T)$ are somewhat deformed (Fig. 11, curves σ_6). This is because the stress σ_6 splits the parameters of interactions J_{11} and J_{13}, as well as J_{12} and J_{14}, since pseudospins "1" and "3", as well as "2" and "4" become nonequivalent. Corresponding order parameters η_1, η_3 and η_2, η_4 also split (Fig. 13).

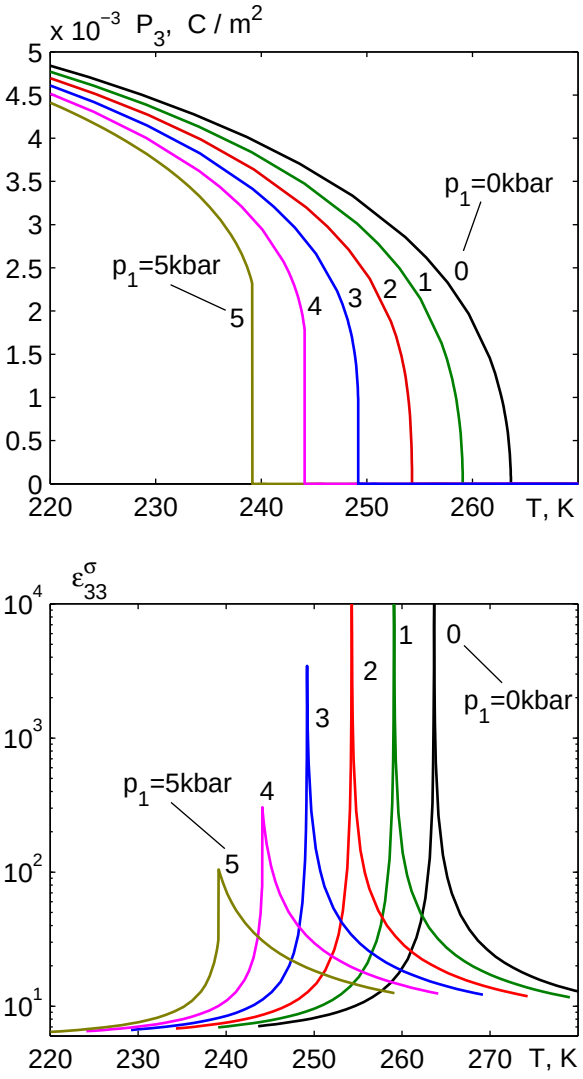

Fig. 12. Temperature dependences of spontaneous polarization P_3 and dielectric permittivity of mechanically free crystal $\varepsilon_{33}^{\sigma}$ at different values of uniaxial pressure p_1.

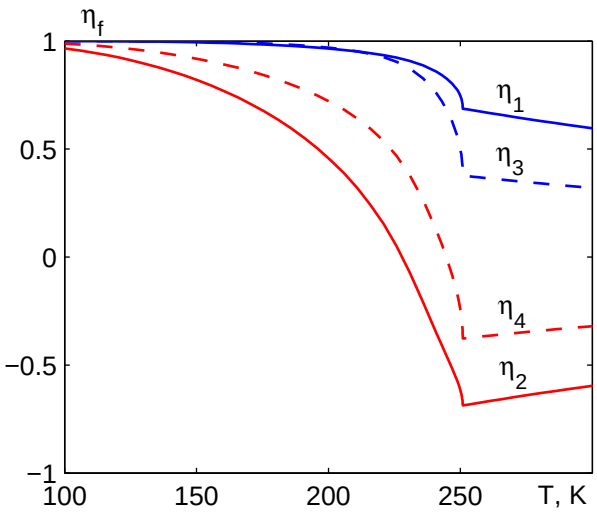

Fig. 13. Temperature dependences of the order parameters η_f at shear stress $\sigma_6 = 5$ kbar.

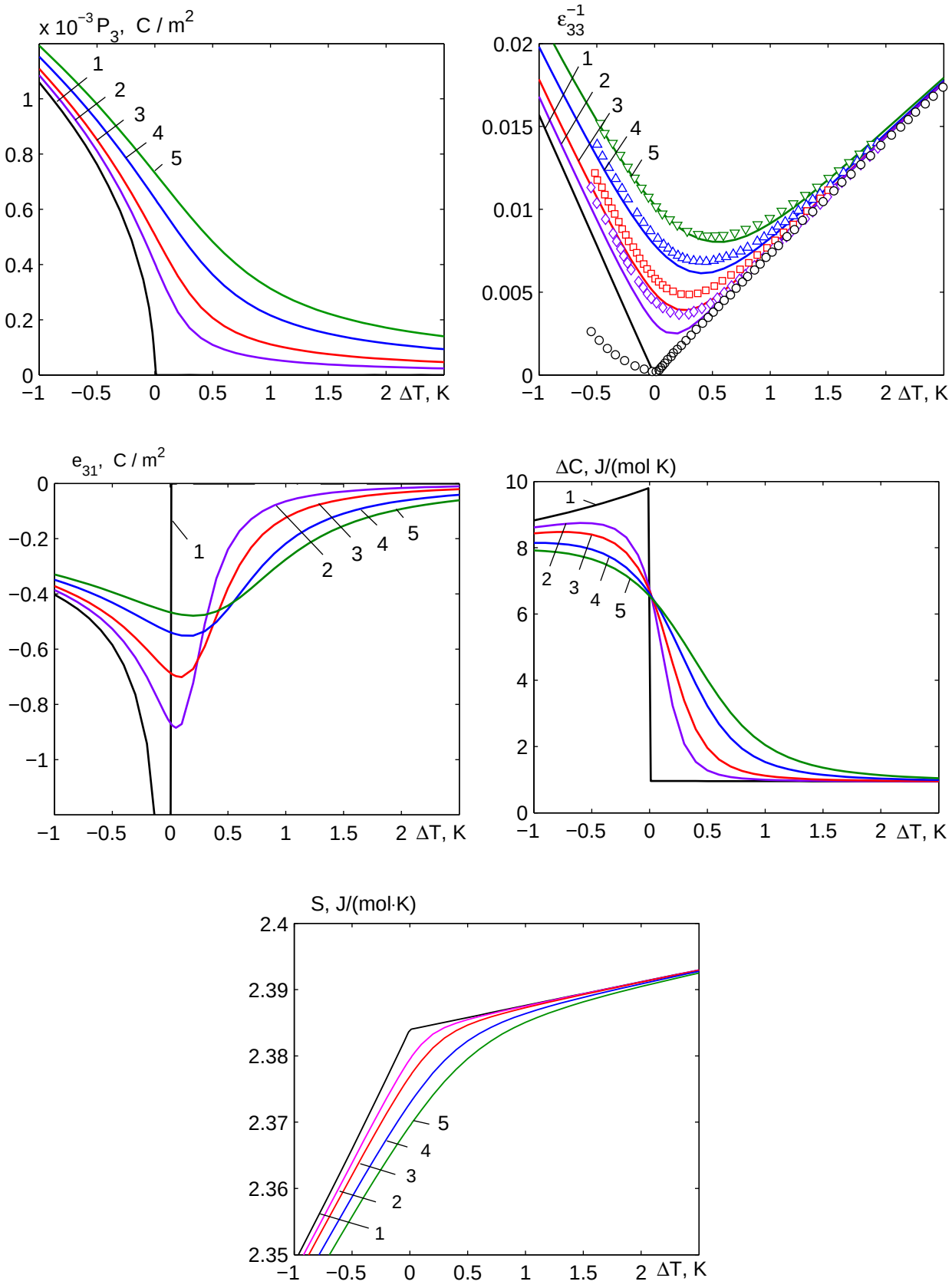

Fig. 14. Temperature dependences of spontaneous polarization P_3, inverse dielectric permittivity of the mechanically free crystal $\varepsilon^{\sigma}_{33}$, piezoelectric coefficients e_{3j} and pseudospin contribution to molar heat capacity ΔC and to molar entropy S at different values of longitudinal electric field E_3 (V/cm): 0 — 1,○; 480 — 2,◇; 950 — 3,□; 1900 — 4,△; 2860 — 5,▽. Symbols are experimental data of [5].

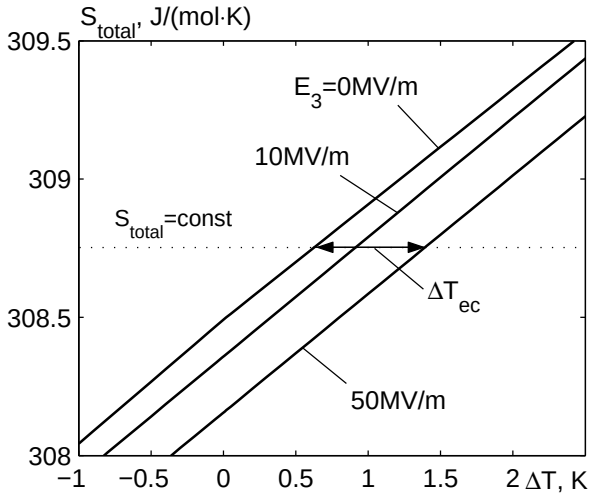

Fig. 15. Temperature dependence of total entropy S_{total} at different values of longitudinal electric field E_3.

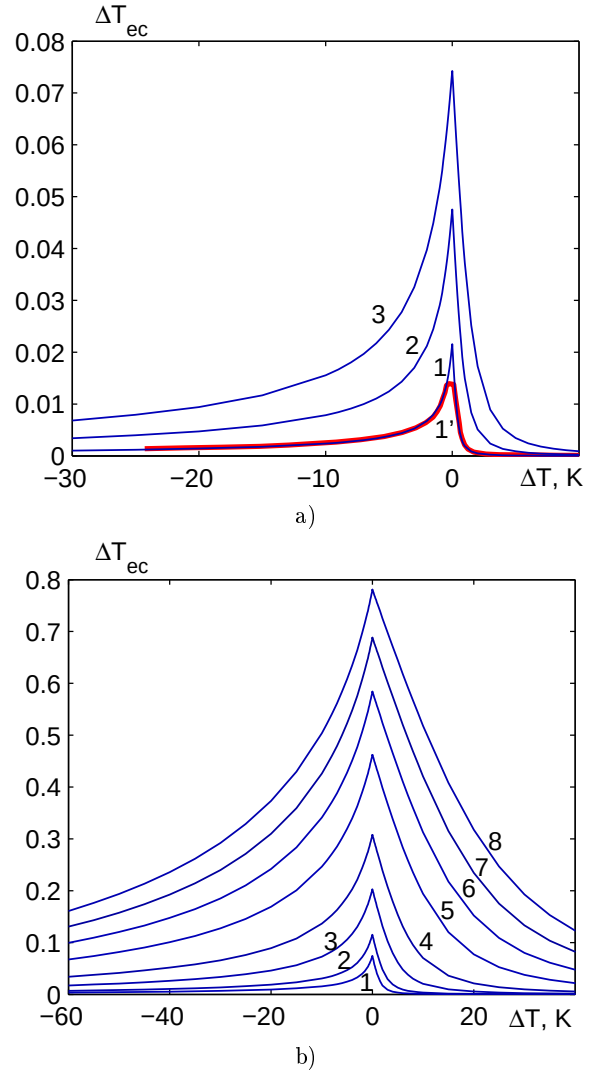

Fig. 16. a) Temperature dependence of electrocaloric change of temperature ΔT_{ec} at weak electric fields E_3 (MV/m): 0.15 — 1,1'[17]; 0.5 — 2; 1.0 — 3; b) Temperature dependence of ΔT_{ec} at strong fields E_3 (MV/m): 1.0 — 1; 2.0 — 2; 5.0 — 3; 10.0 — 4; 20.0 — 5; 30.0 — 6; 40.0 — 7; 50.0 — 8.

The effect of longitudinal electric field E_3 is reduced to smearing of the phase transition. As a result, curves of temperature dependences of thermodynamic characteristics in the external field become smoothed (Fig. 14).

As one can see from this figure, the calculated curves $\varepsilon_{33}^{\sigma}$ at different values of the field satisfactorily agree with experimental data. Therefore this model can be suitable for the investigation of the electrocaloric effect in the $RbHSO_4$ crystal, that is the change of temperature ΔT_{ec} of the crystal at adiabatic (at constant entropy) change of the applied electric field (Fig. 15).

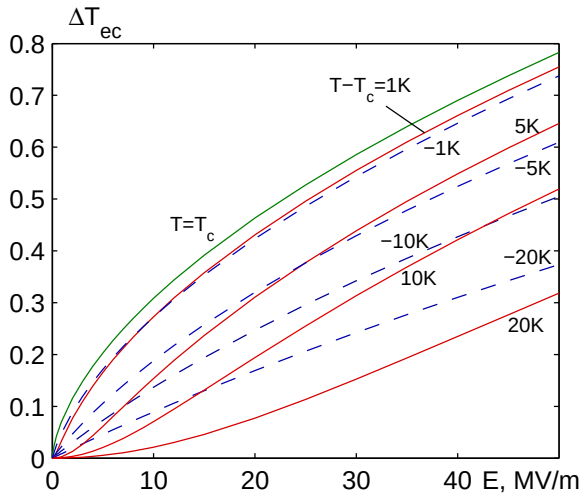

Fig. 17. Field dependence of electrocaloric change of temperature ΔT_{ec} at different values of initial temperature $\Delta T = T - T_{\text{c}}$. Dashed lines correspond to the ferroelectric phase.

The effect of the field on the total entropy S_{total} is less marked, than the effect on the only pseudospin contribution ΔS, because the lattice contribution to the heat capacity stabilizes the electrocaloric change of temperature of the crystal.

Figure 16 shows the dependence of ΔT_{ec} on the initial temperature at different values of adiabatically applied longitudinal field E_3, and Fig. 17 shows the dependence of ΔT_{ec} on the electric field at different initial temperatures.

Thick red curve 1' in Fig. 16 is calculated in [17] using Landau expansion method. In the weak fields ($E_3 < 1$ MV/m) at initial temperature $T = T_{\text{c}}$ the temperature change follows the law $\Delta T_{\text{ec}} \sim E_3^{3/2}$ (green curve in Fig. 17); at $T < T_{\text{c}}$, $\Delta T_{\text{ec}} \sim E_3$ (blue dashed curves in Fig. 17); at $T > T_{\text{c}}$, $\Delta T_{\text{ec}} \sim E_3^2$ (red curves in Fig. 17). At stronger fields $E_3 > 1$ MV/m the dependences $\Delta T_{\text{ec}}(E_3)$ deviate from the mentioned laws and reach saturation at $E_3 \gg 50$ MV/m.

V. CONCLUSIONS

The present model predicts a linearly increasing dependence of temperature T_{c} on hydrostatic p_{h} and uniaxial p_2, p_3 pressures, as well as on shear stress σ_5. The

phase transition remains the second-order one, and the temperature dependences of different thermodynamic characteristics are qualitatively similar, as in the case of absence of stresses.

Uniaxial pressure p_1 linearly lowers the temperature T_c. At small values of the pressures, the phase transition remains the second-order one, but starting from some critical pressure p_1^{cr} the phase transition becomes the first-order one.

Shear stress σ_4 does not influence the calculated thermodynamic characteristics, shear stress σ_6 nearly quadratically lowers the temperature T_c.

The effect of the longitudinal electric field E_3 boils down to smearing the phase transition.

In the weak fields E_3, electrocaloric change of temperature ΔT_{ec} linearly increases with the field in the ferroelectric phase, quadratically — in the paraelectric phase and follows the law $\Delta T_{ec} \sim E_3^{3/2}$ at initial temperature $T = T_c$. At strong fields, the dependencies $\Delta T_{ec}(E_3)$ deviate from the mentioned laws and reach saturation at $E_3 \gg 50$ MV/m.

[1] K. Gesi, K. Ozawa, J. Phys. Soc. Jpn **38**, 459 (1975); https://doi.org/10.1143/JPSJ.38.459.

[2] R. Pepinsky, K. Vedam, Phys. Rev. **117**, 1502 (1960); https://doi.org/10.1103/PhysRev.117.1502.

[3] J. P. Ashmore, H. E. Petch, Can. J. Phys. **53**, 2694 (1975); https://doi.org/10.1139/p75-328.

[4] K. Iton, H. Ohno, S. Kuragaki, J. Phys. Soc. Jpn **64**, 479 (1995); https://doi.org/10.1143/JPSJ.64.479.

[5] E. Nakamura, H. Kajikawa J. Phys. Soc. Jpn **44**, 519 (1978); https://doi.org/10.1143/JPSJ.44.519.

[6] D. H. Blat, V. I. Zinienko, Fiz. Tverd. Tela **18**, 3599 (1976).

[7] R. R. Levitsky, I. R. Zachek, V. I. Varanitsky, Fiz. Tverd. Tela **22**, 2750 (1980).

[8] W. Paprotny, J. Grigas, R. R. Levitsky, I. V. Kutny, V. S. Krasikov, Ferroelectrics **61**, 19 (1984); https://doi.org/10.1080/00150198408018932.

[9] I. R. Zachek, Ya. Shchur, R. R. Levitskii, Physica B **478**, 113 (2015); https://doi.org/10.1016/j.physb.2015.08.058.

[10] I. Stasyuk, O. Velychko, Ferroelectrics **316**, 51 (2005); https://doi.org/10.1080/00150190590963138.

[11] I. R. Zachek, R. R. Levitskii, Ya. Shchur, O. B. Bilenka, Condens. Matter Phys. **18**, 43703 (2015); https://doi.org/10.5488/CMP.18.43703.

[12] I. R. Zachek, R. R. Levitskii, A. S. Vdovych, J. Phys. Stud. **19**, 3703 (2015); https://doi.org/10.30970/jps.19.3703.

[13] I. R. Zachek, R. R. Levitskii, A. S. Vdovych, M. C. Karkuljevska, Phys. Chem. Solid State **16**, 276 (2015); https://doi.org/10.15330/pcss.16.2.276-283.

[14] H. Kajikawa, T. Ozaki, E. Nakamura, J. Phys. Soc. Jpn **43**, 937 (1977); https://doi.org/10.1143/JPSJ.43.937.

[15] M. P. Zajceva, L. A. Shabanova, L. I. Zherebcova, Fiz. Tverd. Tela **21**, 2308 (1979).

[16] K. S. Alexandrov *et al.*, Ferroelectrics **12**, 191 (1976); https://doi.org/10.1080/00150197608241423.

[17] V. S. Bondarev, A. N. Vtyurin, A. S. Krylov, E. M. Kolesnikova, Bull. Reshetnev Siberian State. Aerospace Univ. **5**, 152 (2012).

ПОЛЬОВІ ТА ДЕФОРМАЦІЙНІ ЕФЕКТИ В СЕҐНЕТОЕЛЕКТРИКУ $RbHSO_4$

А. С. Вдович[1], Р. Р. Левицький[1], І. Р. Зачек[2]

[1] *Інститут фізики конденсованих систем НАН України, вул. Свєнціцького, 1, Львів, 79011, Україна*

[2] *Національний університет "Львівська політехніка" вул. С. Бандери 12, 79013, Львів, Україна*

Сеґнетоелектрик із водневими зв'язками $RbHSO_4$ є прикладом кристала, де ефекти тиску суттєві. На відміну від інших сеґнетоелектриків із водневими зв'язками фазовий перехід із високотемпературної парафази в низькотемпературну сеґнетофазу пов'язаний з упорядкуванням не протонів, а сульфатних груп SO_4, які стрибають між двома положеннями рівноваги.

Запропоновано модифіковану чотирипідґраткову псевдоспінову модель сеґнетоелектрика $RbHSO_4$, у якій групам SO_4 приписуються ефективні дипольні моменти і псевдоспіни; а кристал розглядається як система взаємодійних псевдоспінів. Ця модель ураховує п'єзоелектричний зв'язок псевдоспінової підсистеми з деформаціями ґратки, а також зміну симетрії кристала під впливом зсувних напруг σ_4 і σ_6. У наближенні молекулярного поля розраховано спонтанну поляризацію та поздовжню діелектричну проникність механічно затиснутого й вільного кристалів, п'єзоелектричні, пружні та теплові характеристики. Досліджено вплив гідростатичного та одновісних тисків, зсувних напруг та поздовжнього електричного поля на фазовий перехід і фізичні характеристики кристала.

У межах цієї моделі отримано лінійно зростаючу залежність температури T_c від гідростатичного p_h та одновісних p_2, p_3 тисків, а також від зсувної напруги σ_5. При цьому фазовий перехід залишається переходом другого роду, а температурні залежності різних термодинамічних характеристик якісно подібні, як за відсутності механічних напруг. Одновісний тиск p_1 лінійно понижує температуру T_c. При цьому за малих

тисків зберігається перехід другого роду, а, починаючи з деякого критичного тиску $p_1^{\rm cr}$, перехід стає переходом першого роду. Зсувна напруга σ_4 не впливає на розраховані термодинамічні характеристики, зсувна напруга σ_6 понижує температуру $T_{\rm c}$.

Вплив поздовжнього електричного поля E_3 зводиться до розмивання фазового переходу. За слабкого поздовжнього поля E_3 електрокалорична зміна температури $\Delta T_{\rm ec}$ лінійно зростає з полем у сеґнетофазі, квадратично — у парафазі, і за законом $\Delta T_{\rm ec} \sim E_3^{3/2}$ за початкової температури $T = T_{\rm c}$. У сильному полі залежності $\Delta T_{\rm ec}(E_3)$ відхиляються від згаданих законів, а за $E_3 \gg 50$ МВ/м досягають насичення.

Отримано задовільний кількісний опис відповідних експериментальних даних.

Ключові слова: сеґнетоелектрики, діелектрична проникність, п'єзоелектричні коефіцієнти, вплив тиску, вплив електричного поля, електрокалоричний ефект.